Intercalibration of infrared channels of polar-orbiting IRAS/FY-3A with AIRS/Aqua data

Geng-Ming Jiang,[1,2,*]

[1]*Key Laboratory of Wave Scattering and Remote Sensing Information (Ministry of Education), Fudan University, Shanghai 200433, P. R. China*

[2]*State Key Laboratory of Remote Sensing Science, Jointly Sponsored by Beijing Normal University and the Institute of Remote Sensing Applications of Chinese Academy of Sciences, Beijing 100101, P. R. China*

**jianggengming@hotmail.com*

Abstract: This work intercalibrated the infrared window channels 8 (12.47 μm), 9 (11.11 μm) and 19 (3.98 μm) of the InfraRed Atmospheric Sounder (IRAS) aboard the Chinese second generation polar-orbiting meteorological satellite FengYun 3A (FY-3A) with high spectral resolution data acquired by the Atmospheric InfraRed Sounder (AIRS) aboard Aqua. A North Pole study area was selected according to the IRAS and AIRS' viewing geometry. The IRAS/FY-3A L1 data and AIRS/Aqua 1B Infrared geolocated and calibrated radiances (AIRIBRAD) in July of 2008 were used in this work. A sub-pixel registration method was developed and applied to the IRAS and AIRS images to improve the intercalibration accuracy. The co-located measurement pairs were picked out with absolute Viewing Zenith Angle differences less than 5° ($|\Delta VZA|<5°$), absolute Viewing Azimuth Angle differences less than 90° ($|\Delta VAA|<90°$) and absolute time differences less than 15 min ($|\Delta T|<15'$). The results reveal that the convolved AIRS/Aqua measurements are highly linearly related to the IRAS/FY-3A measurements with correlation coefficients greater than 0.93, and calibration discrepancies exist between IRAS and AIRS channels indeed. When the brightness temperatures in IRAS/FY-3A channels change from 230.0 K to 310.0 K, the AIRS-IRAS temperature adjustment linearly varies from −3.3 K to 1.7 K for IRAS/FY-3A channel 8, from −2.9 K to 2.6 K for IRAS/FY-3A channel 9, and from −5.3 K to 1.1 K for IRAS/FY-3A channel 19.

OCIS codes: (280.0280) Remote sensing and sensors; (280.4991) Passive remote sensing.

References and links

1. A. Asem, P. Y. Deschamps, and D. Ho, "Calibration of METEOSAT infrared radiometer using split window channels of NOAA AVHRR," J. Atmos. Ocean. Technol. **4**(4), 553–562 (1987).
2. J. Butler, and R. A. Barnes, "Calibration strategy for the Earth Observation System (EOS)-AM1 platform," IEEE Trans. Geosci. Rem. Sens. **36**(4), 1056–1061 (1998).
3. D. R. Doelling, L. Nguyen, and P. Minnis, "Calibration comparisons between SEVIRI, MODIS and GOES data," In *proc. EUMETSAT Meteorol. Satell. Conf*. Prague, Czech Republic, May 17–20 (2004).
4. D. R. Doelling, P. Minnis, and L. Nguyen, "Calibration comparisons between SEVIRI, MODIS and GOES data," In *Proc. MSG RAO Workshop*. Salzburg, Austria, Sep. 10–11 (2004).
5. P. M. Teillet, J. L. Barker, B. L. Markham, R. R. Irish, G. Fedosejevs, and J. C. Storey, "Radiometric cross-calibration of the Landsat-7 ETM+ and Landsat-5 TM sensors based on tandem data sets," Remote Sens. Environ. **78**(1–2), 39–54 (2001).
6. A. K. Heidinger, C. Cao, and J. T. Sullivan, "Using moderate resolution imaging spectrometer (MODIS) to calibrate advanced very high resolution radiometer reflectance channels," J. Geophys. Res. **107**(D23), 4702 (2002).
7. G. Chander, D. L. Helder, B. L. Markham, J. D. Dewald, E. Kaita, K. J. Thome, E. Micijevic, and T. Ruggles, "Landsat-5 TM reflective-band absolute radiometric calibration," IEEE Trans. Geosci. Rem. Sens. **42**(12), 2747–2760 (2004).
8. G. Chander, D. Meyer, and D. L. Helder, "Cross calibration of the Landsat-7 ETM+ and EO-1 ALI sensor," IEEE Trans. Geosci. Rem. Sens. **42**(12), 2821–2831 (2004).

#120164 - $15.00 USD Received 18 Nov 2009; revised 14 Jan 2010; accepted 20 Jan 2010; published 2 Feb 2010

9. J. F. Le Marshall, J. J. Simpson, and Z. Jin, "Satellite calibration using a collocated nadir observation technique: Theoretical basis and application to the GMS-5 Pathfinder benchmark period," IEEE Trans. Geosci. Rem. Sens. **37**(1), 499–507 (1999).
10. C. J. Merchant, J. J. Simpson, and A. R. Harris, "A cross-calibration of GMS-5 thermal channels against ATSR-2," Remote Sens. Environ. **84**(2), 268–282 (2003).
11. J.-J. Liu, and Z. Li, "A new method for cross-calibration of two satellite sensors," Int. J. Remote Sens. **25**(23), 5267–5281 (2004).
12. E. F. Vermote, and N. Z. Saleous, "Calibration of NOAA16 AVHRR over a desert site using MODIS data," Remote Sens. Environ. **105**(3), 214–220 (2006).
13. M. M. Gunshor, T. J. Schmit, and W. P. Menzel, "Intercalibration of the infrared window and water vapor channels on operational Geostationary Environmental Satellites using a single polar-orbiting satellite," J. Atmos. Ocean. Technol. **21**(1), 61–68 (2004).
14. M. M. Gunshor, T. J. Schmit, W. P. Menzel, and D. C. Tobin, "Intercalibration of broadband geostationary imagers using AIRS," J. Atmos. Ocean. Technol. **26**(4), 746–758 (2009).
15. G.-M. Jiang, H. Yan, and L.-L. Ma, "Intercalibration of SVISSR/FY-2C infrared channels against MODIS/Terra and AIRS/Aqua channels," IEEE Trans. Geosci. Rem. Sens. **47**(5), 1548–1558 (2009).
16. L. Jian, "Introduction of FengYun 3 meteorological satellite," Bimonthly of Xinjiang Meteorology. **29**(4), 45–46 (2006).
17. Y. Liu, T. Hiyama, and Y. Yamaguchi, "Scaling of land surface temperature using satellite data: A case examination on ASTER and MODIS products over a heterogeneous terrain area," Remote Sens. Environ. **105**(2), 115–128 (2006).

1. Introduction

Intercalibration is an operation that relates the outputs of a given sensor, in a certain spectral channel, to the output of one or more sensors measured in other channels [1,2]. The commonly used intercalibration approaches are the Ray-Matching (RM) method [3–8], the Radiative Transfer Modeling (RTM) method [9–12], and the High Spectral Convolution (HSC) method [13–15]. Their advantages and disadvantages were detailed in [15].

FengYun-3A (FY-3A), launched on May 27, 2008, is the Chinese second generation polar-orbiting meteorological satellite. On FY-3A, there are a total of 11 payloads, and one is the InfraRed Atmospheric Sounder (IRAS). It cross-track scans the Earth surface with 26 channels covering from visible to infrared and the nominal spatial resolution is 17 km at nadir [16]. The IRAS/FY-3A channels 8 (12.47 μm), 9 (11.11 μm), 19 (3.98 μm) and 20 (3.76 μm) are four window bands located in the infrared spectrum, and the Noise Equivalent Temperature differences (NEΔT) are not greater than 0.12 K (Table 1). Figure 1 displays the spectral responses of the four window channels. The measurements in the four window channels can be used in many applications, such as the retrievals of Earth surface temperature and emissivity. Consequently, the on-orbit characteristics of the IRAS/FY-3A instrument are essential in providing long-term and accurate measurements, however its operational calibration has not been validated yet.

Table 1. Spectral characteristics of the four IRAS/FY-3A infrared window channels

No.	Name	Central wavelength (μm)	NEΔT at 300 K (K)	Maximum limit (K)	Main gaseous absorber or window
8	IR8	12.47	0.11	330	Window
9	IR9	11.11	0.12	330	Window
19	IR19	3.98	0.07	340	Window
20	IR20	3.76	0.07	340	Window

The Atmospheric InfraRed Sounder (AIRS) is an instrument aboard the EOS Aqua polar-orbiting satellite, containing 2,378 infrared channels from 3.74 to 15.39 μm and four visible/near-infrared channels. The infrared radiance data product is stable to 10 mK/year and accurate to better than 250 mK, which is the most accurate and stable set of high spectral infrared measurements made in space to date (http://daac.gsfc.nasa.gov/AIRS). Because of its high spectral resolution and high accuracy, the AIRS/Aqua infrared radiances can be used to intercalibrate the infrared channels of other instruments, if they have overlapped channels. This method has been successfully applied to intercalibrating the instruments aboard geostationary satellites [13–15]. As shown in Fig. 1, the IRAS channels 8, 9 and 19 are fully covered by the AIRS infrared channels, while only part of IRAS channel 20 is covered by the

#120164 - $15.00 USD Received 18 Nov 2009; revised 14 Jan 2010; accepted 20 Jan 2010; published 2 Feb 2010

AIRS spectrum. Therefore, it is a good choice to calibrate IRAS/FY-3A channels 8, 9 and 19 with the AIRS/Aqua infrared data. However, because both IRAS and AIRS are aboard polar-orbiting satellites, rare IRAS and AIRS observations satisfy the strict matching conditions as used in [15].

This work aimed at the intercalibration of IRAS/FY-3A infrared window channels 8, 9 and 19 with high spectral resolution AIRS/Aqua data using the HSC method. In the following, four sections will be presented. Section 2 recalls the HSC method; Section 3 describes the study area, satellite data and data processing. Section 4 demonstrates the results, and the final section is devoted to the summary and conclusion.

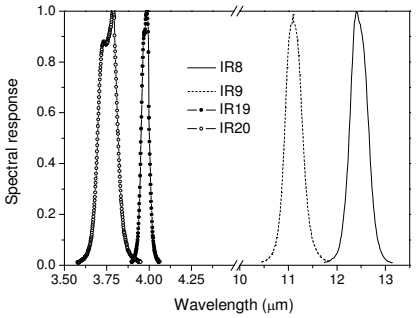

Fig. 1. Spectral responses of IRAS/FY-3A channels 8, 9, 19 and 20

2. Method

The HSC method was first developed to intercalibrate the geostationary imagers with high spectral resolution data [14], and then was improved in [15]. The HSC method not only possesses the advantages of both RM and RTM methods, but also overcomes their disadvantages. Here, the HSC method is recalled below.

Under the coincident, co-angled and co-located conditions, the measurement in a conventional channel i, R_i, can be expressed through the convolution of high spectral resolution data with the Spectral Response Function (SRF) of that channel

$$R_i = \int_{\lambda_1}^{\lambda_2} f_i(\lambda) R_\lambda(n) d\lambda \Big/ \int_{\lambda_1}^{\lambda_2} f_i(\lambda) d\lambda \qquad (1)$$

where $f_i(\lambda)$ is the SRF of channel i, λ_1 and λ_2 are the minimum and maximum wavelengths of the SRF, respectively, $R_\lambda(n)$ is the radiance in a high spectral channel n at wavelength λ. R_i is also called the convolved radiance.

As pointed out in [15], the HSC method works only for the conventional channels fully covered by the high spectral channels.

3. Study area, data description and processing

Because of the homogeneity, the relatively flat surface, and the well-known emissivity, sea is an ideal calibration site [1,3,4,10]. In the work of [15], a tropical area was chosen as study area in terms of the instruments' viewing geometry. However, this does not work because both of IRAS and AIRS are aboard the polar-orbiting satellites (the minimum absolute time difference of the co-located IRAS/FY-3A and AIRS/Aqua measurements exceeds 3.0 h). As we know, the observations of a location in a day by a polar-orbiting satellite are decided by its latitude: higher the latitude, the more observations. To minimize the absolute time differences, the most suitable study area is located in the polar region. In this work, a North Pole area shown in Fig. 2 was selected as the study area. Besides the Arctic Ocean, Asia, North America, Europe and Greenland are partially or fully contained in the study area.

#120164 - $15.00 USD Received 18 Nov 2009; revised 14 Jan 2010; accepted 20 Jan 2010; published 2 Feb 2010

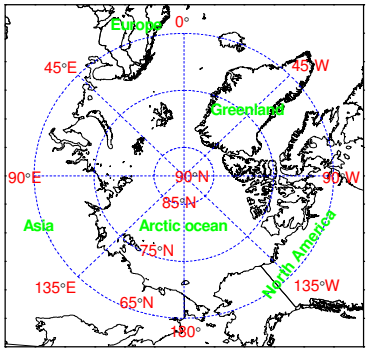

Fig. 2. Study area

In the polar region, as we know, the perpetual days and the perpetual nights alternate every six months. Because of the solar irradiation, the Earth surface temperatures in the perpetual days are usually higher than the ones in the perpetual nights, leading to the observations in the perpetual days to have much wider dynamic range than the ones in the perpetual nights, which is beneficial to intercalibration. Therefore, a time span from July 1 to July 31 of 2008 was considered.

The IRAS/FY-3A L1 data and the AIRS/Aqua 1B Infrared geolocated and calibrated radiances (AIRIBRAD) during the time span and covering the study area, a total of 395 IRAS data files and 1,407 AIRS data files, were downloaded from the FengYun Satellite Remote Sensing Data Services Website (http://fy3.satellite.cma.gov.cn/) and the Goddard Earth Sciences Data and Information Services Center (http://disc.sci.gsfc.nasa.gov/AIRS/), respectively. The brightness temperatures in IRAS/FY-3A channels 8, 9 and 19 and the AIRS radiances in the channels covering the IRAS channels were, respectively, extracted from the IRAS/FY-3A L1 data and the AIRS infrared level 1B data. Longitude, latitude, Viewing Zenith Angle (VZA), Viewing Azimuth Angle (VAA) and observation time were also extracted from the two data sets. The AIRS radiances were convolved with the SRFs of IRAS channels 8, 9 and 19 (Fig. 1) using Eq. (1) to simulate the IRAS/FY-3A observations, and then converted into brightness temperature using radiance-temperature look-up tables.

Before further processing, a Cartesian coordinate system was built in this way: the North Pole (90°N) is taken as the origin, the x-axis varies from 90°E to 90°W, and the y-axis changes from 180° to 0° (Fig. 1). To convert the longitude (θ) and latitude (φ) in degree into the Cartesian coordinate system, the following equation was used

$$\begin{cases} x = (90-\varphi)\cos\zeta \\ y = (90-\varphi)\sin\zeta \end{cases} \tag{2}$$

with $\zeta = \begin{cases} \vartheta + 90, & \text{if } \vartheta \le 270^{\circ} \\ \vartheta - 270, & \text{if } \vartheta > 270^{\circ} \end{cases}$ and $\vartheta = \begin{cases} \theta, & \text{if } \theta \ge 0^{\circ} \\ \theta + 360, & \text{if } \theta < 0^{\circ} \end{cases}$.

After the coordinate system transfer, the range of the study area changes from –30.0 to 30.0 for both x-axis and y-axis, and then the coordinate system transferred data were re-sampled with Δx = 2.0 and Δy = 2.0 by the Inverse Distance Weighting (IDW) method. The sizes of the re-sampled images are 31 × 31.

The re-sampled images acquired by IRAS/FY-3A and AIRS/Aqua need further accurate coordinate registration. This can be done using the minimum Root-Mean-Square (RMS) error difference [15]. However, the coordinate registration results may be not good for such coarse resolution images in this work, and the sub-pixel registration method is much better: firstly, the images were amplified by a factor of 10, then accurate coordinate registration was carried out to obtain the x- and y-offsets according to the amplified images, and finally one of the two images before amplification was re-sampled according to the x- and y-offsets using the bi-

#120164 - $15.00 USD Received 18 Nov 2009; revised 14 Jan 2010; accepted 20 Jan 2010; published 2 Feb 2010

linear interpolation method. The re-sampling process was conducted on radiance instead of temperature to avoid the error caused by surface heterogeneity [17].

For this special case, the following criteria were used to find out the co-located measurements pairs between IRAS and AIRS observations: the absolute VZA differences less than 5.0° (|ΔVZA|<5.0°), the absolute VAA differences less than 90° (|ΔVAA|<90°), and absolute time differences less than 15 min (|ΔT|<15').

4. Results

The total number of the qualified measurement pairs in July of 2008 with |ΔVZA|<5.0°, |ΔVAA|<90° and |ΔT|<15' is 1180. Figure 3 displays the distribution of the |ΔVZA|, |ΔVAA| and |ΔT| of these measurement pairs. Both the |ΔVZA| and |ΔT| are evenly distributed, and the frequency is ~20%, while the |ΔVAA| is mainly distributed within the range from 45° to 60°.

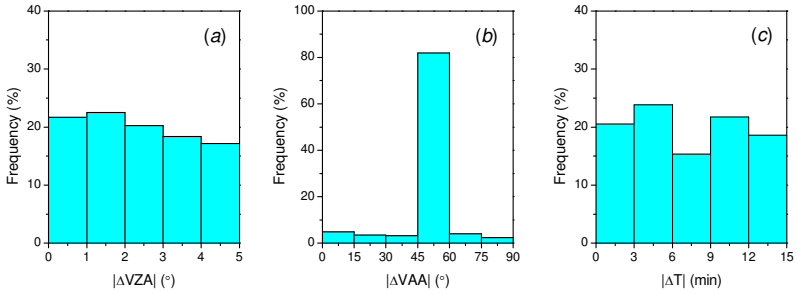

Fig. 3. Histograms of the |ΔVZA| (left), |ΔVAA| (middle) and |ΔT| (right)

Then, the measurement pairs of brightness temperature in K were drawn in a Cartesian coordinate system (Fig. 4). As we know, the WMO-lead program for intercalibration called GSICS (Global Space-based Inter-Calibration System) limits the time between observations to 5 min, and only 440 pairs satisfy their criteria (Red crosses in Fig. 4). In this work, no significant difference was observed between the measurement pairs with |ΔT|<5 min and with |ΔT|<15 min, hence the 15 min criteria was reasonably adopted. Figure 4 illustrates that the convolved AIRS/Aqua measurements are linearly related to the IRAS/FY-3A measurements with correlation coefficients greater than 0.94, and calibration discrepancies exist between IRAS and AIRS channels. The use of the sub-pixel registration reduced the linear fitting RMS (Root-Mean-Square) errors by ~1.0 K, and final RMS errors are ~2.0 K. The large standard deviation may due to the relatively loose criteria. When the brightness temperatures in IRAS channels change from 230.0 K to 310.0 K, the AIRS-IRAS temperature adjustment (difference between the convolved AIRS brightness temperature and the IRAS brightness temperature in the same channel) linearly varies from −3.3 K to 1.7 K for IRAS/FY-3A channel 8, from −2.9 K to 2.6 K for IRAS/FY-3A channel 9, and from −5.3 K to 1.1 K for IRAS/FY-3A channel 19. When measurement pairs of radiances in $mW/m^2\text{-}sr\text{-}cm^{-1}$ were used, they are also highly linearly related with correlation coefficients greater than 0.93 and RMS errors of 2.859, 2.912 and 0.0473 for IRAS/FY-3A channels 8, 9 and 19 respectively. The linear fitting results may be used to recalibrate the data in IRAS/FY-3A channels 8, 9 and 19 for the whole temperature/radiance range, and the results are given below for convenience:

$$T_{8,\mathrm{R}} = 1.063 \times T_8 - 17.80 \quad \text{or} \; I_{8,\mathrm{R}} = 1.0539 \times I_8 - 5.649 \tag{3}$$

$$T_{9,\mathrm{R}} = 1.069 \times T_9 - 18.76 \quad \text{or} \quad I_{9,\mathrm{R}} = 1.0687 \times I_9 - 5.127 \tag{4}$$

$$T_{19,\mathrm{R}} = 1.079 \times T_{19} - 23.44 \quad \text{or} \quad I_{19,\mathrm{R}} = 1.04165 \times I_{19} - 0.0466 \tag{5}$$

#120164 - $15.00 USD Received 18 Nov 2009; revised 14 Jan 2010; accepted 20 Jan 2010; published 2 Feb 2010

where X_8, X_9 and X_{19}, respectively, stand for the BTs in Kelvin ($X = T$) or the radiances in mW/m^2-sr-cm^{-1} ($X = I$) at top-of-atmosphere in IRAS channels 8, 9 and 19 directly extracted from the IRAS/FY-3A L1 data, while $X_{8,R}$, $X_{9,R}$ and $X_{19,R}$ represent the intercalibrated BTs ($X = T$) or radiances ($X = I$) in IRAS/FY-3A channels 8, 9 and 19 respectively.

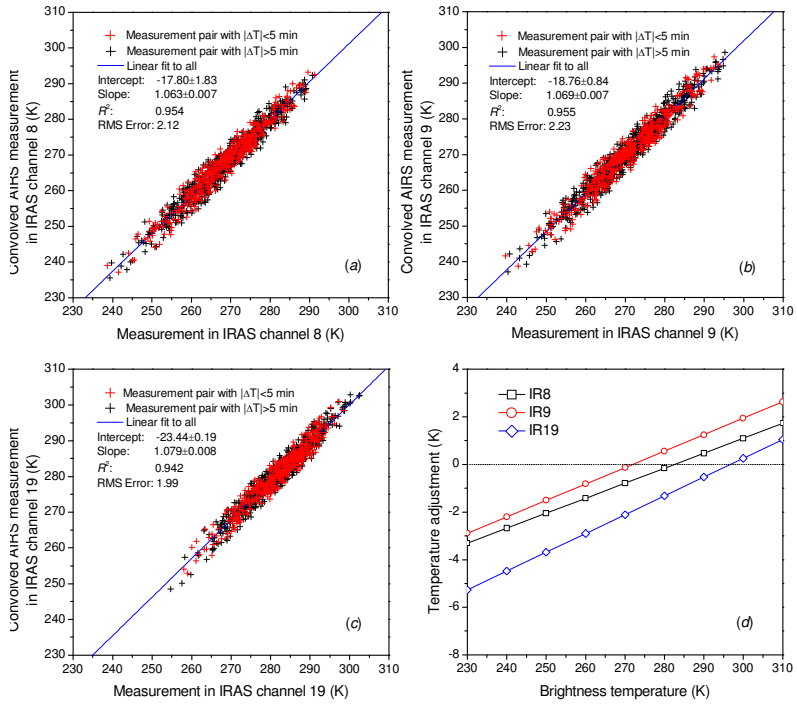

Fig. 4. Measurement pairs between IRAS and AIRS and the linear fitting results (a total of 1180 measurement pairs; RMS denotes Root-Mean-Square)

5. Summary and conclusion

This work addressed the intercalibration of the infrared window channels 8, 9 and 19 of IRAS aboard the polar-orbiting satellite FY-3A with the high spectral resolution AIRS/Aqua data using the HSC method. The IRAS/FY-3A L1 data and the AIRS/Aqua 1B infrared geolocated and calibrated radiances in July of 2008 and covering the North Pole study area were used, and sub-pixel registration between the IRAS and AIRS images were implemented to improve the intercalibration accuracy. A total of 1180 measurement pairs were qualified with $|\Delta VZA|<5.0°$, $|\Delta VAA|<90°$ and $|\Delta T|<15$ min.

The results indicate that the convolved AIRS/Aqua measurements are highly linearly related to the IRAS/FY-3A measurements, and intercalibration discrepancies exist between IRAS and AIRS channels. When the brightness temperatures in IRAS channels change from 230 K to 310 K, the AIRS-IRAS temperature adjustment linearly varies from −3.3 K to 1.7 K for IRAS channel 8, from −2.9 K to 2.6 K for IRAS channel 9, and from −5.3 K to 1.1 K for IRAS channel 19.

Acknowledgments

This work was jointly funded by the Open Foundation of the State Key Laboratory of Remote Sensing Science, Jointly Sponsored by Beijing Normal University and the Institute of Remote Sensing Applications of Chinese Academy of Sciences (2009KFJJ018), and the Fudan University Foundation for Young Scholars (08FQ06).